2024 IEEE Haptics Symposium (HAPTICS)
April 7-10, 2024. Long Beach, California, USA

Richer Textural Information in the Horizontal Component of the Contact Force Compared with the Normal Component

Ayaka Tamura[1] and Shogo Okamoto[1]

***Abstract*— Most surface texture displays provide either vibrotactile or variable-friction stimuli to users through finger pads, and they control the changes in the contact force either along the normal or tangential direction. This study aimed to answer a fundamental question: that is, which of the two force components contains the most textural information. We measured the contact force when a fingertip slid over 21 types of materials. The force was decomposed into tangential and normal components to compute individual power spectra. Two classification machines, Fisher's discriminant analysis and a support vector machine, were used to categorize the materials based on the power spectra. They confirmed that the tangential component of the contact force was more helpful in distinguishing the 21 materials, with an average success rate of 29%. In contrast, this proportion was as low as 21% when the normal force was used to train and test the machines. Furthermore, this proportion did not improve substantially, even when the two components were used together. Although these classification machines employ principles different from those of humans, these results suggest that humans may rely more on the tangential component of the contact force than on the normal component to judge textures. These results motivate us to compare the two force components in terms of different aspects in the future.**

I. Introduction

Touch panels are the most representative human–computer interface, and surface texture displays, which provide tactile stimuli to their users, enhance user experience [1]. Most existing display techniques employ vibrotactile stimuli [2]–[4], variable-friction stimuli [5]–[8], or conjunct stimuli [9]–[11]. Vibrotactile displays actuate a touch panel or the entire chassis to deform the finger pad in contact. The vibration direction is limited to the normal or horizontal directions. Variable-friction displays are further categorized into electrostatic [5], [6] and ultrasound vibration types [7], [12]. Both approaches dynamically control the surface friction of the touch panels; hence, the horizontal contact force is primarily controlled. Thus, surface texture displays typically impart a change in the contact force to the finger pad along the normal or tangential direction.

Here, the following question is raised: which of the tangential and normal components of the contact force are more effective in presenting textures. To date, some studies have addressed this question. Biggs and Srinivasan [13] compared these two directions from the viewpoint of the difference in the stiffness of the finger pad between the longitudinal and perpendicular directions and the properties of the actuators delivering skin stimuli. However, to the best of our knowledge, no previous studies have answered the question regarding the perceptual quality of textures, whereas several studies have shown that tactile stimuli in either direction can deliver textural information (e.g., [2], [3], [14]–[17]). For example, Wiertlewski et al. [2] demonstrated that the tangential components include sufficient information to discriminate between several different surface features. When a stylus is used to explore textured surfaces, vibrotactile stimuli along the longitudinal direction of the stylus can effectively present various textures [16]. However, these studies did not directly answer our question because they did not directly compare normal and tangential force components. By contrast, Ito et al. [18] and Otake et al. [9] compared vibrotactile stimuli normal to the fingertip and electrostatic friction stimuli to present virtual grating scales on touch panels. Although they concluded that the best realism was achieved when the two types of stimuli were combined, the vibrotactile condition was more suitable than the electrostatic condition when only one condition was used. However, grating scales are only a small part of the texture variety sought by numerous researchers.

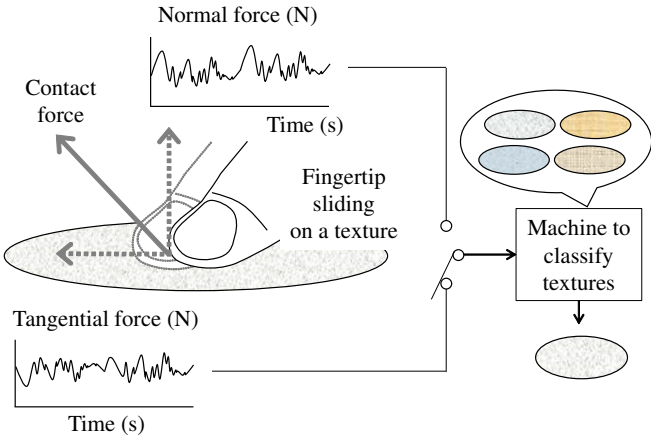

Fig. 1. Scheme of the study to compare normal and tangential contact forces to classify textures

The objective of this study was to determine whether tangential or normal forces are more potent in presenting textures from one aspect. As shown in Fig. 1, the normal and tangential contact forces caused by sliding the fingertips on various textures were measured. The time-series information was then converted into frequency spectra. Machine-learning algorithms were used to estimate the type of material that produces these spectra. Subsequently, the

[1]TAMURA Ayaka and OKAMOTO Shogo are with the Department of Computer Science, Tokyo Metropolitan University, Japan. okamotos@tmu.ac.jp

979-8-3503-4511-7/24/$31.00 ©2024 IEEE

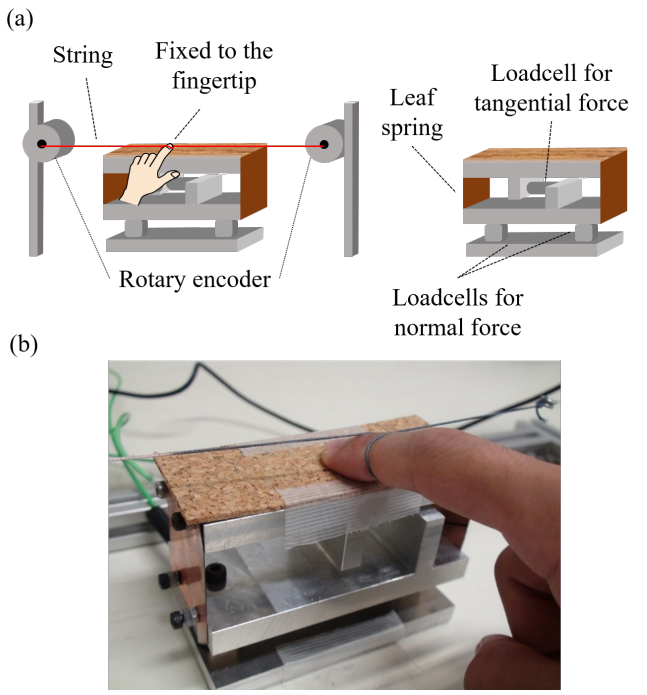

Fig. 2. Instruments to measure the contact force and finger motion. (a) Schematic. (b) Photo. Adapted from [20].

classification performances of the two directional forces were compared. Although earlier studies have shown that the frequency spectra of the contact forces contain rich textural information [19], [20], no study has compared the forces along the two directions. Determining which directional component retains more textural information will deepen our understanding of the tactile recognition of textures and help in designing surface texture displays.

II. Methods

A. Apparatus

We used an instrument [20] shown in Fig. 2 to measure the finger position and the tangential and normal components of the finger contact force when a finger slid over the materials. The main components of the force measurement instrument were a crystal-type loadcell for the tangential component (9217A, Kistler, Switzerland) and two loadcells for the normal component (9313AA2, Kistler). The signals from the loadcells were conditioned using charge amplifiers (5073A and 5015, Kistler, Switzerland) and were recorded at 2 kHz using a data acquisition box (NI USB-6211, National Instruments Corp., TX). The finger position was measured using two rotary encoders with a string-winding system (MLS-12, Microtech Laboratory Inc., Japan; nominal resolution: 0.04 mm). The winding system retains the tension of the string using a constant-force spring system embedded in the product. The two encoders were aligned on the right and left sides of the instrument, and their spring forces canceled each other. The string was fixed to the finger at the distal interphalangeal joint.

B. Participants

The participants were seven university students (two women) in their 20s who provided informed consent prior to the experiment. The participants were unaware of the study objectives.

C. Specimens: Twenty-one materials

Twenty-one types of materials shown in Fig. 3 were used in the study. They included four wooden (medium-density fiber) grating scales cut using a laser cutter, with the wavelength λ of 0.75 mm or 1.0 mm, and the width of the groove of 0.2 mm or 0.4 mm. Other materials included cloth, felt, paper, fake leather, fake woven straw, wood, artificial grass, aluminum sheets, and artificial skin (Bioskin; Beaulax Co., Ltd., Japan). All the materials were cut into 11 cm $\times$ 4 cm pieces.

D. Procedures

The individual participants wiped their index fingers with a paper towel. They then slid their index finger on each material fixed on the instrument described in Section II-A. Only the finger pad was in contact with the material. The participants attempted to maintain a sliding speed ranging from 75 to 125 mm/s with feedback from an experimenter. The measurement lasted 20 s, such that sufficient contact force data at the designated sliding speed were available for the analysis described in Section II-E. No instructions were provided to the participants regarding contact force. The participants were not blinded and could view the material during the measurement process.

E. Data analysis

We used continuous 300-ms periods of force data, during which the finger speed was in the range of 75–125 mm/s. Five such 300-ms intervals were extracted for each combination of individual participants and materials. Hence, 105 (five intervals $\times$ 21 materials) sample intervals were used for the individuals. For each interval, the power spectra of the tangential (f_t) and normal (f_n) components were computed using the fast Fourier transform. The first 100 frequency components, which correspond to 3.33–333 Hz, were used for the latter analysis. We did not use the DC component because it contains information on the individual magnitude of the contact force rather than that specific to the material surfaces. The mean power was calculated for every two frequency components. For example, the power values for 3.33 and 6.66 Hz were averaged. Subsequently, the values of the 100 frequency components were reduced to 50 values. Hence, each sample contained these 50 power values and was used for the machine-learning approaches.

As mentioned in Section I, the objective of this study was to compare the tangential and normal components of the contact force. Nonetheless, it is meaningful to set the other conditions as references. Two additional conditions involving both components were prepared. In one condition, we computed the power spectra of the coefficient of friction. We

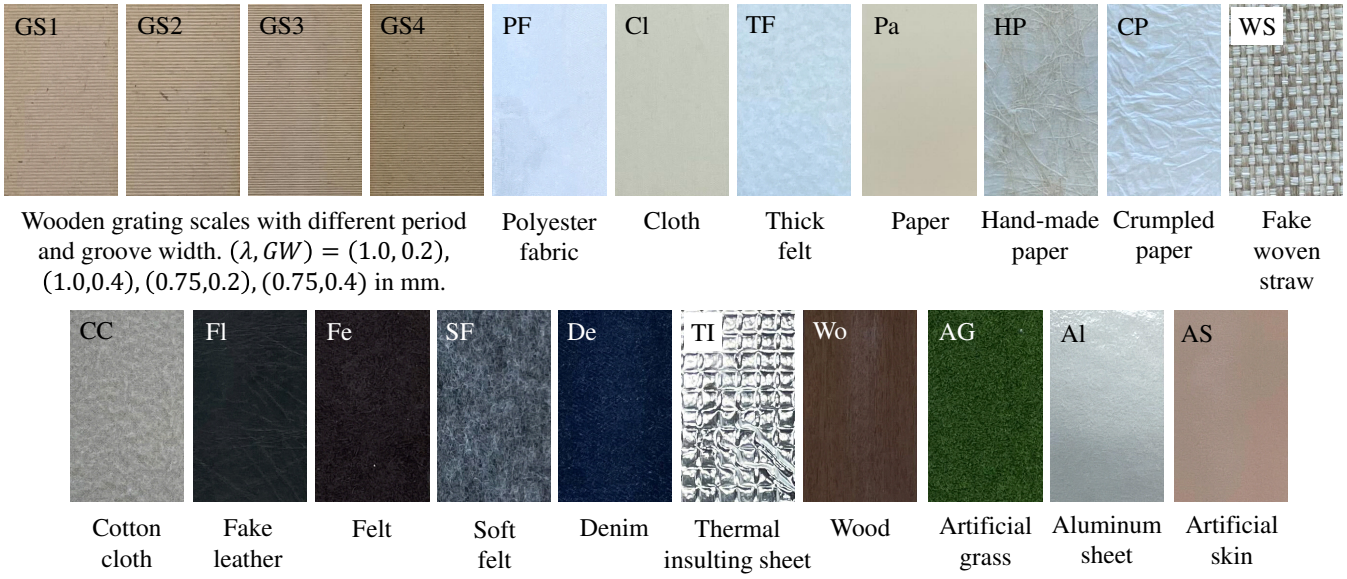

Fig. 3. Twenty-one materials used in the study

divided the tangential component into a normal component at each moment and calculated the time series of μ-values:

$$\mu(t) = \frac{f_t(t)}{f_n(t)}. \quad (1)$$

The power spectrum of the time series of $\mu(t)$ values was computed for each sampling interval of 300 ms. Another condition is the combination of f_t and f_n. As previously mentioned, there are 50 power values for each f_t and f_n. Twenty-five power values were extracted from each of f_t and f_n, and then, they were combined into a new sample with 50 power values. For this process, every two frequency components of the spectra of f_t and f_n were used.

Hence, we compare four conditions: f_t, f_v, μ, and the conjunct (f_t and f_v). For each condition, each sample contained 50 machine-learning variables or dimensions.

Fisher's discriminant analysis, also known as linear discriminant analysis, and a support vector machine were used to classify the samples into 21 categories. The computational conditions for each method are as follows.

Fisher's discriminant analysis is a supervised version of principal component analysis. The bases of the principal component space are determined such that the ratio of the variance between classes (materials) and that within individual classes is maximized along the individual bases. Consequently, each basis is sensitive to the difference between classes but less sensitive to the differences among the samples in the same class. The model was tested using cross-validation. The principal component space was established using 104 of the 105 samples for each participant. The remaining samples were tested in established spaces. The sample was categorized as one of the 21 materials using the k-nearest neighbor method, with $k = 7$. The seven nearest samples to the tested sample were selected in the principal component space, and the category of the sample was determined through voting by these seven samples. This process was repeated for all 105 samples. The hyperparameters, that is, the number of principal components and k, were determined to be two and seven, respectively, such that the average classification performance among all the participants was maximized. The classification model was trained and tested for each participant and the four conditions, among which the available force component cues were different.

For the support vector machine, we used the *ClassificationECOC* model in MATLAB (2023b, MathWorks Inc., MA). This model addresses multiclass categorization problems. In our problem setting, the support vector machine tested the model in a 10-fold cross-validation manner. Similar to Fisher's discriminant analysis, for individual participants, each of the four types of force cues, namely f_t, f_n, μ, and (f_t and f_n), was examined to classify the materials.

III. Results

Tables I and II list the correct classification proportions for Fisher's discrimination analysis and the support vector machine, respectively. They show the proportions of the different force cues for each individual. The mean values for the seven participants are shown. The number of materials was 21, and the chance was 4.8% ($1/21 \sim 0.048$).

The results of the two machine-learning algorithms largely agreed with each other. The tangential force cues led to higher correct classification proportions for the two algorithms than the normal force cues. For Fisher's discrimination analysis, the proportions of the tangential force cues f_t were not significantly different from those of the normal force cues f_n (signed-rank statistics $T = 21$, $p = 0.30$, signed-rank test without p-value adjustment). For the support vector machine, the proportions for f_t were significantly greater than those for f_n (signed-rank statistics $T = 28$, $p = 0.016$, signed-rank test without p-value adjustment).

TABLE I

FISHER'S DISCRIMINANT ANALYSIS: CORRECT CLASSIFICATION PROPORTIONS (%) OF MATERIALS FOR DIFFERENT FORCE CUES

Participant	Tangential (f_t)	Normal (f_n)	Friction coeff. (μ)	Tan. & norm. (f_h and f_n)
1	25.71	9.52	11.43	15.24
2	21.90	29.52	11.43	26.67
3	25.71	10.48	13.33	16.19
4	23.81	10.48	13.33	19.05
5	11.43	9.52	18.10	20.95
6	5.71	10.48	10.48	16.19
7	15.24	10.48	7.62	20.00
Mean	18.50	12.93	12.25	19.18

TABLE II

SUPPORT VECTOR MACHINE: CORRECT CLASSIFICATION PROPORTIONS (%) OF MATERIALS FOR DIFFERENT FORCE CUES

Participant	Tangential (f_t)	Normal (f_n)	Friction coeff. (μ)	Tan. & norm. (f_h and f_v)
1	24.76	15.24	21.90	21.90
2	36.19	32.38	30.48	46.67
3	32.38	22.86	26.67	39.05
4	26.67	12.38	22.86	21.90
5	35.24	28.57	22.86	38.10
6	15.24	13.33	16.19	20.00
7	34.29	20.95	27.62	31.43
Mean	29.25	20.82	24.08	31.29

These results suggest that tangential force cues are more effective for distinguishing between different materials. Furthermore, the proportions of the coefficient of friction μ were marginally smaller than those of f_t (signed-rank statistics: $T = 27$, $p = 0.0312$ for the support vector machine, with no p-value adjustment).

The conjunctive ($f_t + f_n$) and tangential force (f_t) cues exhibited better classification performance than the friction (μ) and normal force (f_n) cues. This trend was more clearly observed for the support vector machine. For Fisher's discriminant analysis, this trend was also observed; however, the correct classification proportions were smaller than those of the support vector machine by approximately 10%. Hence, the differences in the proportions of the different cues are obscure.

Fig. 4 shows the distribution of the samples in the first–second principal component plane for one participant. This shows the loci of the 105 samples (five replications $\times$ 21 samples) computed by using Fisher's discriminant analysis with tangential force components f_t. In this figure, all 105 samples were used to compute the model. Five samples collected from the same material, i.e, five same symbols, are closely placed; however, they are not completely distinguished from the samples of different materials. Fig. 5 shows the loadings of the first and second principal components computed for the same participant. These values correspond to the weighting coefficients of the tangential-force frequency components.

Table III shows the confusion matrix of the materials when the support vector machine, which exhibited better performance than Fisher's discriminant analysis, was used

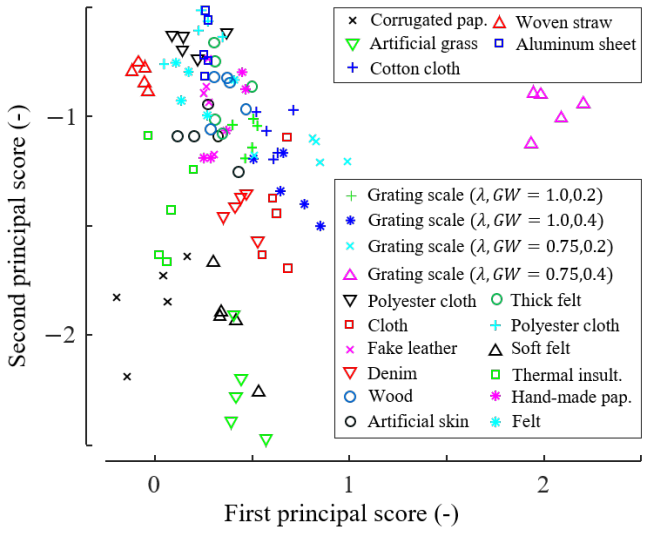

Fig. 4. Loci of materials on the principal component plane for a certain participant. Each material has five samples because it was explored five times.

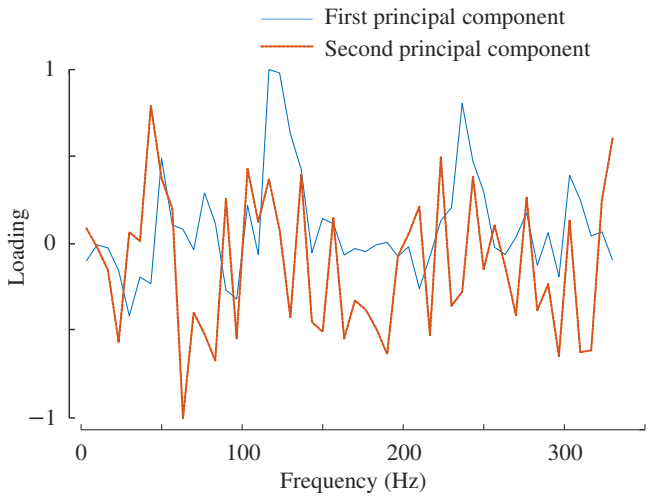

Fig. 5. Example of principal loadings of the first and second principal components. Computed from the tangential forces of 105 samples for one participant, which are the same as the data in Fig. 4.

to categorize the materials with the spectra of the tangential forces as cues. It lists the number and type of materials into which the samples of each material were categorized.

IV. DISCUSSION

One of the reasons we adopted Fisher's discriminant analysis was that it allowed us to interpret the principal components based on their loadings. We expected the principal component space to be linked to the human perceptual dimensions, as in [21]. However, as in Fig. 5, which shows the loadings of the principal components for the tangential force, the loadings largely fluctuate above and below the zero levels. For example, the loading of the second principal component is approximately -0.5 at 216.7 Hz. This value was approximately 0.5 at 218.3 Hz. These two components

TABLE III

CONFUSION MATRIX OF MATERIAL CLASSIFICATION FOR ALL THE PARTICIPANTS. SUPPORT VECTOR MACHINE AND TANGENTIAL COMPONENTS OF THE CONTACT FORCES WERE USED. THE SUM OF NUMBERS IN EACH ROW IS 35 (5 SAMPLES × 7 PARTICIPANTS). THE DIAGONAL ELEMENTS ARE THE NUMBERS OF CORRECT CLASSIFICATION. THE SYMBOLS OF THE MATERIALS, SUCH AS GS1, MATCH THOSE IN FIG. 3.

		Estimated material																			
		GS1	GS2	GS3	GS4	PF	Cl	TF	CC	Fe	FL	SF	De	TI	Wo	Pa	HP	CP	WS	AG	Al	AS
Actual material	GS1	6	5	3	1	1	2	0	3	1	2	0	4	0	1	1	3	1	1	0	0	0
	GS2	11	10	2	1	0	0	0	1	0	0	0	1	0	0	1	1	2	1	0	2	2
	GS3	4	2	11	2	0	3	0	4	1	0	0	1	0	2	0	2	1	0	1	1	0
	GS4	2	2	9	12	0	2	1	2	1	0	1	2	0	1	0	0	0	0	0	0	0
	PF	1	0	0	0	12	0	0	2	2	3	0	0	1	3	5	0	0	2	0	3	1
	Cl	1	1	1	0	0	13	6	1	4	0	0	3	0	5	0	0	0	0	0	0	0
	TF	0	1	1	0	0	4	5	4	3	1	0	2	0	4	1	2	0	2	0	2	3
	CC	3	1	1	0	1	3	3	10	4	0	0	0	0	1	0	1	0	2	1	1	3
	Fe	0	0	0	0	0	0	2	4	11	0	0	1	0	7	1	1	0	2	0	2	4
	FL	1	0	0	0	2	0	2	1	3	7	1	0	0	1	8	1	0	0	0	1	7
	SF	1	2	0	0	0	0	0	0	0	0	11	4	1	0	0	0	0	2	14	0	0
	De	1	1	1	0	0	2	2	0	1	0	2	9	1	4	1	5	0	1	3	0	1
	TI	1	0	0	0	1	0	3	2	2	4	1	2	9	2	1	1	0	4	0	2	0
	Wo	0	0	0	0	2	3	5	3	2	1	0	1	0	15	0	0	0	0	0	1	2
	Pa	1	0	0	0	6	0	0	0	1	5	0	0	0	2	14	0	0	0	0	6	0
	HP	0	0	0	0	0	1	3	1	3	0	2	2	1	3	0	12	1	0	6	0	0
	CP	1	0	0	0	0	0	0	0	0	0	4	4	3	0	0	6	12	1	4	0	0
	WS	1	0	0	0	2	0	3	1	2	1	3	1	3	1	0	0	0	11	3	2	1
	AG	0	0	0	0	0	1	0	0	1	0	2	7	0	2	0	4	1	3	11	3	0
	Al	0	0	0	0	2	0	2	0	3	3	0	0	2	0	7	1	0	1	3	7	4
	AS	0	0	0	0	1	0	1	4	1	5	0	2	0	4	1	1	0	1	0	7	7

play different roles in distinguishing materials, although they are separated merely by 1.6 Hz. Such extremely fluctuating loadings may not pertain to the frequency characteristics of the human tactile system, whose sensitivity draws moderate curves along the frequency axis [22]. The principal components of Fisher's discriminant analysis were optimized to categorize the materials, and it is unlikely that the principal components suggest the perceptual aspects of material judgment. To connect machine-learning algorithms and human tactile systems, it may be better to employ supervised methods based on the results of perceptual experiments [23]–[25]. In contrast to Fisher's discriminant analysis, the support vector machine is less explainable, and we may not be able to discuss the connections between a machine's criteria of material judgment and human tactile perception.

Nonetheless, the classification results of machine-learning algorithms reflect human perception to some extent. Table III shows that certain materials are frequently confused with each other. In particular, two grating scales (GS1 and GS2) were misclassified. Furthermore, artificial grass (AG) and soft felt (SF) were confused with each other. A closeup of the four materials is shown in Fig. 6. These materials exhibit subjectively similar tactile textures if their surfaces are explored. Hence, machine-learning algorithms and human tactile systems share some features, which partly endorse the suggestion of the study; that is, the tangential component includes more helpful information for judging textures than the normal component.

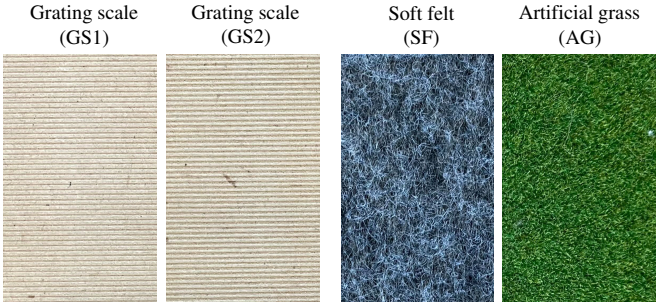

Fig. 6. Closeups of four materials. The support vector machine frequently confused GS1 and GS2, and SF and AG. These pairs of materials exhibit similar tactile textures.

V. CONCLUSION

To determine whether the tangential or normal components of the contact force produced by a sliding finger include more information for discriminating textures, we compared the performances of their power spectra to categorize 21 materials. For classification, two machine-learning approaches, namely, Fisher's discriminant analysis and a support vector machine, were employed. The categorization performances of the two force components were largely consistent between the two learning methods. The tangential components exhibited a significantly better performance, indicating that they contained richer information than the normal components. This study did not involve perceptual experiments that could be referred to by classification algorithms. Further studies on human psychophysical performance are necessary to support this conclusion.

ACKNOWLEDGMENT

This study was partially supported by MEXT Kakenhi 23H04360 and 20H04263.

REFERENCES

[1] X. Sun, C. Zhang, and G. Liu, "Improved tactile perception of 3D geometric bumps using coupled electrovibration and mechanical vibration stimuli," *The Computer Journal*, vol. 65, no. 3, pp. 621–630, 2020.

[2] M. Wiertlewski, J. Lozada, and V. Hayward, "The spatial spectrum of tangential skin displacementcan encode tactual texture," *IEEE Transactions on Robotics*, vol. 27, no. 3, pp. 461–472, 2011.

[3] Y. Matsuura, S. Okamoto, S. Asano, H. Nagano, and Y. Yamada, "A method for altering vibrotactile textures based on specified materials," in *IEEE International Symposium on Robot and Human Interactive Communication*. IEEE, 2012, pp. 995–1000.
[4] S. Asano, S. Okamoto, Y. Matsuura, H. Nagano, and Y. Yamada, "Vibrotactile display approach that modifies roughness sensations of real textures," in *IEEE International Symposium on Robot and Human Interactive Communication*, 2012, pp. 1001–1006.
[5] R. Haghighi Osgouei, J. R. Kim, and S. Choi, "Improving 3D shape recognition with electrostatic friction display," *IEEE Transactions on Haptics*, vol. 10, no. 4, pp. 533–544, 2017.
[6] J. Mullenbach, M. Peshkin, and J. E. Colgate, "eshiver: Lateral force feedback on fingertips through oscillatory motion of an electroadhesive surface," *IEEE Transactions on Haptics*, vol. 10, no. 3, pp. 358–370, 2017.
[7] S. Ghenna, E. Vezzoli, C. Giraud-Audine, F. Giraud, M. Amberg, and B. Lemaire-Semail, "Enhancing variable friction tactile display using an ultrasonic travelling wave," *IEEE Transactions on Haptics*, vol. 10, no. 2, pp. 296–301, 2017.
[8] K. Otake, S. Okamoto, Y. Akiyama, and Y. Yamada, "Tactile texture rendering for electrostatic friction displays: Incorporation of low-frequency friction model and high-frequency textural model," *IEEE Transactions on Haptics*, vol. 15, no. 1, pp. 68–73, 2022.
[9] ——, "Tactile texture display combining vibrotactile and electrostatic-friction stimuli: Substantial effects on realism and moderate effects on behavioral responses," *ACM Transactions on Applied Perception*, vol. 19, no. 4, p. 18.
[10] S. Ryu, D. Pyo, B.-K. Han, and D.-S. Kwon, "Simultaneous representation of texture and geometry on a flat touch surface," in *Haptic Interaction*, S. Hasegawa, M. Konyo, K.-U. Kyung, T. Nojima, and H. Kajimoto, Eds. Singapore: Springer Singapore, 2018, pp. 83–86.
[11] G. Liu, C. Zhang, and X. Sun, "Tri-modal tactile display and its application into tactile perception of visualized surfaces," *IEEE Transactions on Haptics*, vol. 13, no. 4, pp. 733–744, 2020.
[12] Z. Cai and M. Wiertlewski, "Ultraloop: Active lateral force feedback using resonant traveling waves," *IEEE Transactions on Haptics*, vol. 16, no. 4, pp. 652–657, 2023.
[13] J. Biggs and M. A. Srinivasan, "Tangential versus normal displacements of skin: Relative effectiveness for producing tactile sensations," in *Proceedings of IEEE Symposium On Haptic Interfaces For Virtual Environment and Teleoperator Systems*, 2002, pp. 121–128.
[14] L. Winfield, J. Glassmire, J. E. Colgate, and M. Peshkin, "T-pad: Tactile pattern display through variable friction reduction," *Proceedings of The Second Joint EuroHaptics Conference and Symposium on Haptic Interfaces for Virtual Environment and Teleoperator Systems*, pp. 421–426, 2007.
[15] S. Saga and R. Raskar, "Simultaneous geometry and texture display based on lateral force for touchscreen," *Proceedings of the IEEE World Haptics Conference*, pp. 437–442, 2013.
[16] H. Culbertson and K. J. Kuchenbecker, "Importance of matching physical friction, hardness, and texture in creating realistic haptic virtual surfaces," *IEEE Transactions on Haptics*, vol. 10, no. 1, pp. 63–74, 2017.
[17] J. Jiao, Y. Zhang, D. Wang, Y. Visell, D. Cao, X. Guo, and X. Sun, "Data-driven rendering of fabric textures on electrostatic tactile displays," in *IEEE Haptics Symposium*, 2018, pp. 169–174.
[18] K. Ito, S. Okamoto, Y. Yamada, and H. Kajimoto, "Tactile texture display with vibrotactile and electrostatic friction stimuli mixed at appropriate ratio presents better roughness textures," *ACM Transactions on Applied Perception*, vol. 16, no. 4, p. 20, 2019.
[19] M. Wiertlewski, C. Hudin, and V. Hayward, "On the 1/f noise and non-integer harmonic decay of the interaction of a finger sliding on flat and sinusoidal surfaces," *Proceedings of the IEEE World Haptics Conference*, pp. 25–30, 2011.
[20] H. Hasegawa, S. Okamoto, and Y. Yamada, "Phase difference between normal and shear forces during tactile exploration represents textural features," *IEEE Transactions on Haptics*, vol. 13, no. 1, pp. 11–17, 2020.
[21] S. Okamoto, H. Nagano, and Y. Yamada, "Psychophysical dimensions of tactile perception of textures," *IEEE Transactions on Haptics*, vol. 6, no. 1, pp. 81–93, 2013.
[22] S. J. Bolanowski, G. A. Gescheider, R. T. Verrillo, and C. M. Checkosky, "Four channels mediate the mechanical aspects of touch," *Journal of Acoustic Society of America*, vol. 84, no. 5, pp. 1680–1694, 1988.
[23] W. M. Bergmann Tiest and A. M. L. Kappers, "Analysis of haptic perception of materials by multidimensional scaling and physical measurements of roughness and compressibility," *Acta Psychologica*, vol. 121, no. 1, pp. 1–20, 2006.
[24] K. Higashi, S. Okamoto, Y. Yamada, H. Nagano, and M. Konyo, "Hardness perception based on dynamic stiffness in tapping," *Frontiers in Psychology*, vol. 9, p. 2654, 2019.
[25] Y. Matsuura, S. Okamoto, H. Nagano, and Y. Yamada, "Multidimensional matching of tactile sensations of materials and vibrotactile spectra," *Information and Media Technologies*, vol. 9, no. 4, pp. 505–516, 2014.